

Frank Schultz, Vera Erbes, Sascha Spors, Stefan Weinzierl

# Derivation of IIR prefilters for soundfield synthesis using linear secondary source distributions

**Conference paper | Published version**

This version is available at <https://doi.org/10.14279/depositonce-8769>



Schultz, Frank; Erbes, Vera; Spors, Sascha; Weinzierl, Stefan (2013): Derivation of IIR prefilters for soundfield synthesis using linear secondary source distributions. In: AIA-DAGA 2013 : proceedings of the International Conference on Acoustics ; 18 - 21 March 2013 in Merano. Berlin: Deutsche Gesellschaft für Akustik e.V. pp. 2372–2375.

## Terms of Use

Copyright applies. A non-exclusive, non-transferable and limited right to use is granted. This document is intended solely for personal, non-commercial use.

**WISSEN IM ZENTRUM**  
**UNIVERSITÄTSBIBLIOTHEK**

Technische  
Universität  
Berlin

# Derivation of IIR prefilters for soundfield synthesis using linear secondary source distributions

Frank Schultz<sup>1</sup>, Vera Erbes<sup>2</sup>, Sascha Spors<sup>1</sup>, Stefan Weinzierl<sup>2</sup>

<sup>1</sup> Institute of Communications Engineering, Universität Rostock, R.-Wagner-Str. 31 (H8), D-18119 Rostock, Germany

<sup>2</sup> Audio Communication Group, TU Berlin, Einsteinufer 17c, D-10587 Berlin, Germany

E-Mail: {frank.schultz,sascha.spors}@uni-rostock.de, {v.erbes,stefan.weinzierl}@tu-berlin.de

## Introduction

Typical applications of 2.5-dimensional wave field synthesis (WFS) [1] can be realized with a very efficient and straightforward signal processing chain. For high frequencies and large distances of the virtual primary source and the listener to the secondary source distribution (SSD) wave field synthesis can be considered as a spatially fullband delay-and-sum method. The driving function thus consists of a specific amplitude factor and a specific delay (i.e. a frequency dependent phase shift) per individual secondary source [1, eq. (27), (37)], [2, eq. (25)], [3, eq. (29)]) and a so called prefilter. The infinite SSD features -3 dB/octave low-pass characteristics in the farfield, cf.  $\circ$  in fig. 1. The prefilter with the transfer function

$$H_{\text{Pre}}(\omega) = \sqrt{j\omega} = \sqrt{\omega} e^{+j\frac{\pi}{4}} \quad (1)$$

has +3 dB/octave high-pass characteristics with a frequency independent phase shift of  $45^\circ$  and is minimum-phase. It compensates the frequency response of the line source in 2.5-dimensional sound field synthesis. This is realized by filtering the prefilter spectrum with the virtual source spectrum. Note that the prefilter does not depend on an individual secondary source in this case which makes this computation step in WFS very efficient. In literature the prefilter is also referred to as a fractional order system or a half-derivative system [4]. Filter design realizations and methods for the ideal half-derivative are most notably published in the field of control engineering. In practical realizations the SSD is of finite length and is spatially sampled with the secondary source distance  $\Delta x$ . This has consequences on the required characteristics of the prefilter. Due to the spatial sampling of the continuous SSD additional propagating spatial aliasing contributions may arise in the temporal frequency response at the receiver point. For the reproduction of a plane wave using an infinite, linear and discretized SSD the anti-aliasing condition with speed of sound  $c$  in m/s, plane wave radiation angle  $0 \leq \theta_{\text{PW}} \leq \pi$  and the frequency  $f$  in Hz reads

$$f < \frac{c}{\Delta x (1 + |\cos \theta_{\text{PW}}|)} \quad (2)$$

[3, eq. (38)]. Note that the anti-aliasing condition changes when employing other virtual sources and SSDs of different finite length. In [2] it was shown that the temporal frequency response of the aliasing contribution can be averaged to about +3 dB/octave when considering a receiver point far away from the SSD.

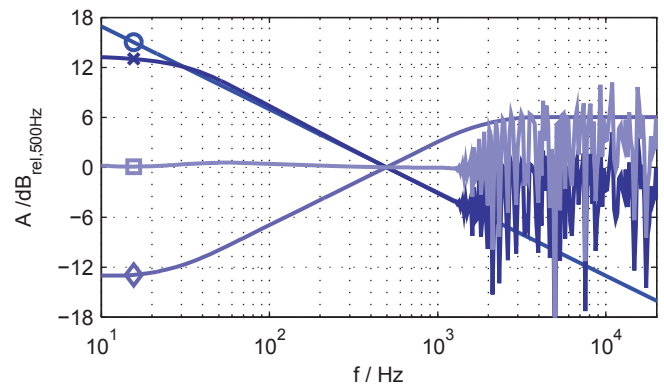


**Figure 1:** Amplitude frequency responses for plane wave 2.5D-synthesis:  $\circ$ : infinite, continuous, linear SSD in the far field;  $\times$ : finite, discrete, linear SSD (length: 40 m, secondary source spacing  $\Delta x = 0.4$  m, listener reference point 20 m away from SSD center);  $\diamond$ : prefilter;  $\square$ : compensation result.

Hence the customized prefilter must not amplify this energy further but rather leave the frequency range unaffected. Furthermore, due to the finite length of the SSD the frequency response smoothly flattens out for low frequencies. In fig. 1 the temporal frequency response for a finite and discretized SSD which synthesizes a plane wave with  $\theta_{\text{PW}} = \pi/2$  is shown for a receiver point 20 m away from the middle axis of the SSD. In the uncompensated spectrum ( $\times$ ) the additional aliasing energy contribution above 1.5 kHz and the low frequency deviation can be observed. The customized prefilter thus must feature shelving filter characteristics ( $\diamond$ ) and is able to compensate to an almost flat spectrum ( $\square$ ). Note that a subwoofer coupling is straightforward when employing the shelving characteristics in the low frequencies.

## IIR Filter Design

Most realizations of sound field synthesis implement the driving function as finite-impulse response filters (FIR, i.e. non-recursive system [5]), which then includes frequency dependent amplitude, phase and delay per individual secondary source. WFS however requires only a gain and delay per secondary source. The impulse response of the prefilter has to be convolved only once with the virtual source signal. The prefilter may be implemented as a FIR filter with the phase term  $\phi = -\omega\tau + \pi/4$  for a chosen constant delay time  $\tau$  to realize a causal system. To further reduce the computational complexity the use of recursive filters (usually referred to as infinite impulse response (IIR) [5]) of very low

order will be proposed here. In a different approach an IIR filter design for WFS was introduced in [6] for the prefilter and the fractional delay following [4]. It was shown that 5<sup>th</sup> and 6<sup>th</sup> order IIR filters match the desired amplitude response of the ideal prefilter reasonably well for the given simulations. However, the design methods [4, 6] for the ideal half-derivative are not feasible for the shelving prefilter characteristic proposed here. A straightforward customization of the shelving prefilter with very few degrees of freedom is required as the frequency response heavily depends on application specific parameters, such as the employed virtual source and the SSD. The filter design is performed in the frequency domain. The filter is parameterized with the two shelving frequencies  $f_{\text{Low}}$  and  $f_{\text{Aliasing}}$  at which the transition from the ideal +3 dB/octave slope towards the specific flat curve segment should occur. The discontinuity between adjacent curve segments is then smoothed in order to make the following optimization problem more robust. Therefore, a frequency range

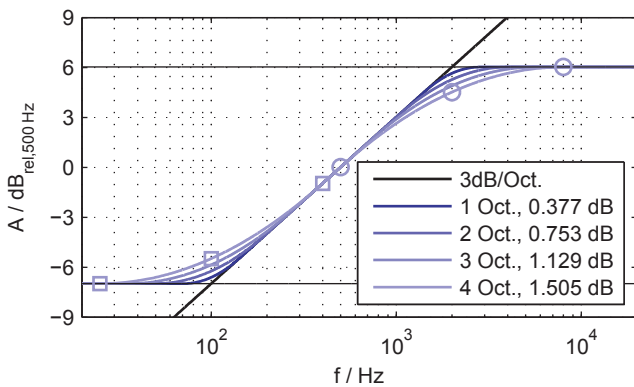


**Figure 2:** Amplitude frequency response of +3 dB/octave shelving prefilter with individual 3-point Lagrange interpolation for  $f_{\text{Low}}=100$  Hz ( $\square$ ) and  $f_{\text{Aliasing}}=2$  kHz ( $\circ$ ) with different bandwidths. The markers belong to interpolation points for the transition bandwidth of four octaves. The dB-values state the specific offset of the middle interpolation point  $P(f_2, A_2)$  regarding the ideal +3 dB/oct. slope.

in terms of typical audio filter bandwidth is defined for each of the two frequencies, cf. fig. 2. Between the three points  $P(\log_{10}(f_{1,2,3}), A_{1,2,3})$  in dB at which either  $f_2 = f_{\text{Low}}$  or  $f_2 = f_{\text{Aliasing}}$ , a smooth amplitude response is realized with the Lagrange interpolation (§3.3 [7]) for curve values  $[\log_{10}(f), A]$  in dB. The remaining unknown amplitude quantity  $A_2$  in dB results from demanding a perfect smooth transition between adjacent curve segments (i.e. the flat or the +3 dB/octave slope must concatenate with the Lagrange polynomial exactly). To achieve that the first derivative of the 2<sup>nd</sup> order Lagrange polynomial has to be evaluated and matched. Fig. 2 exemplarily shows the shelving prefilter with Lagrange interpolation using different bandwidths for the frequencies  $f_{\text{Low}}=100$  Hz and  $f_{\text{Aliasing}}=2$  kHz. Note that the amplitude quantity  $A_2$  diverges more from the ideal +3 dB/octave slope for larger bandwidths. Since it is known that the ideal +3 dB/octave slope prefilter with +45° phase is minimum-phase by itself

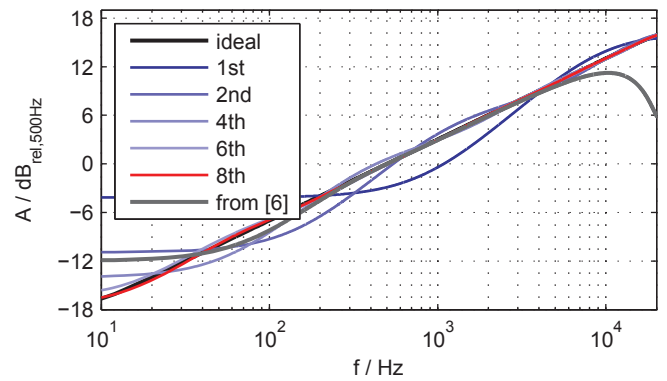


**Figure 3:** Amplitude frequency response for  $f_{\text{Low}}=8$  Hz and  $f_{\text{Aliasing}}=32$  kHz, different IIR filter orders, two octaves Lagrange interpolation bandwidth, in comparison: 6<sup>th</sup> order IIR from [6].

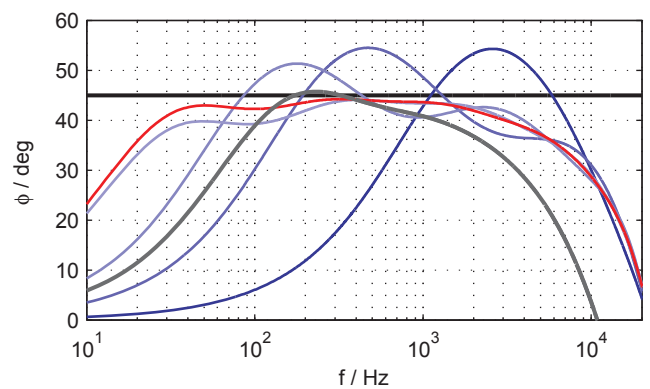


**Figure 4:** Phase frequency response for fig. 3.

it appears valid and straightforward to require also minimum-phase characteristics for the shelving prefilters. The compensation of the phase for frequencies above the spatial aliasing frequency is not required due to the indeterminate phase. Furthermore, it may not be a feasible approach to correct the phase response perfectly in the low frequencies since this would require very high order and potentially unstable IIR filters as the minimum-phase characteristics should then converge to a more complex phase behavior. The Matlab optimization algorithm `iirlpnorm` [5] with default parameterization was used to design minimum-phase IIR filters based on the predefined amplitude frequency response (e.g. fig. 2) with 1 Hz resolution and the sampling frequency  $f_s=48$  kHz.

## Filter Design Examples

Some examples are given within this section to present the performance of the proposed design method. At first, consider the frequencies  $f_{\text{Low}}=8$  Hz and  $f_{\text{Aliasing}}=32$  kHz for which a two octaves Lagrange interpolation bandwidth is applied. The frequencies were chosen in order to create an almost ideal +3 dB/octave slope within the audio frequency range for a quasi-continuous and infinite SSD. In fig. 3 and 4 the amplitude frequency response and phase frequency response, respectively is shown for different IIR filter orders. Furthermore, the

IIR filter proposed in [6] is plotted for comparison. As can be seen in the figures the IIR filters of 6<sup>th</sup> and 8<sup>th</sup> order matches the amplitude response very well combined with a phase response which is approaching the desired +45° phase shift for a very wide frequency range. Due to the flat frequency response at the lower and upper frequencies the minimum-phase characteristics forces the phase to 0°. The 1<sup>st</sup> to 4<sup>th</sup> order IIR filters do not match the required target frequency response very well. When

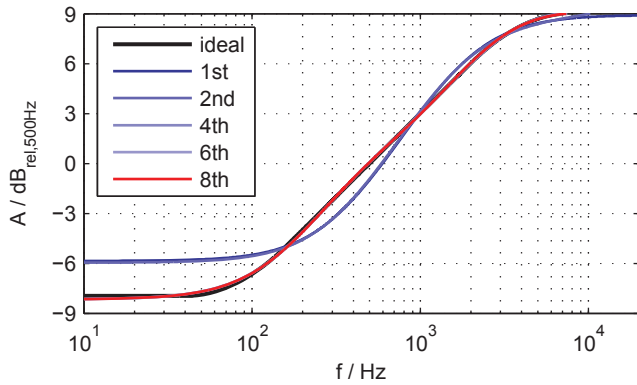


**Figure 5:** Amplitude frequency response for  $f_{Low}=80$  Hz and  $f_{Aliasing}=4$  kHz, different IIR filter orders, two octaves Lagrange interpolation bandwidth.

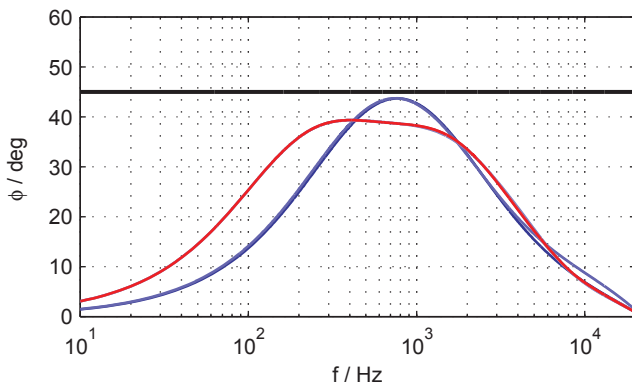


**Figure 6:** Phase frequency response for fig. 5.

comparing the 6<sup>th</sup> order filter from [6] the conclusion may be permissible that the filter design method proposed here is superior in terms of better matched amplitude and phase. Another example is presented in fig. 5, 6 for the frequencies  $f_{Low}=80$  Hz and  $f_{Aliasing}=4$  kHz. The 1<sup>st</sup> and 2<sup>nd</sup> as well as the 4<sup>th</sup>, 6<sup>th</sup> and 8<sup>th</sup> order IIRs show comparable performance which means that for the higher order versions additional poles and zeros are redundant for the desired filter characteristics. Hence a 4<sup>th</sup> order IIR filter would perfectly match the amplitude response whereas the phase approaches a constant-like shift about 37° for the mid frequencies. It is worth to note that the range and the absolute value of the constant-like phase shift has been decreased in comparison to the first example due to a more narrow frequency range at which the +3 dB/octave slope is applied. The 1<sup>st</sup> and 2<sup>nd</sup> order IIR filters do not match the target amplitude very well while approaching the exact 45° phase only for very few frequencies. A third example can be considered as a very

special case. Consider the frequencies  $f_{Low}=125$  Hz and  $f_{Aliasing}=2$  kHz which could be typical for a real world WFS array. When choosing a bandwidth of two octaves the frequency ranges at which the individual Lagrange interpolation is applied are directly concatenated at  $f=500$  Hz. Hence, the amplitude response of the shelving filter becomes point symmetric. In fig. 7 and 8 it can easily be seen that for this example even a 1<sup>st</sup> order minimum-phase IIR filter provides a well matched target amplitude. Interestingly, a highshelf filter of 1<sup>st</sup> order with the Laplace transfer function

$$H_{Shelve,1st\ order}(s = \sigma + j\omega) = g_2 \frac{\frac{\sqrt{g_1}}{\omega_c} s + 1}{\frac{1}{\omega_c \sqrt{g_1}} s + 1} \quad (3)$$

and  $\omega_c = 2\pi \cdot 500$  rad/s,  $g_1 = 4$  and  $g_2 = 0.5$  can be used for this prefilter characteristic.

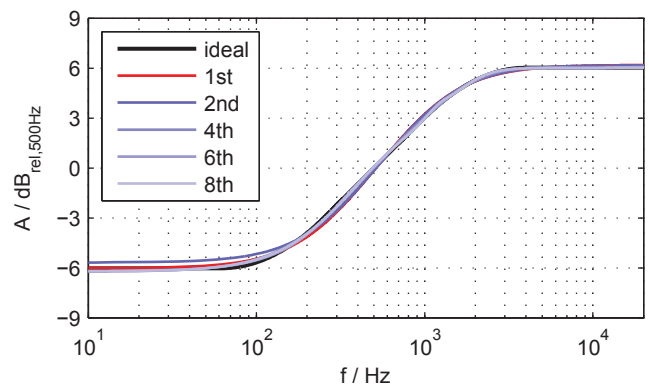


**Figure 7:** Amplitude frequency response for  $f_{Low}=125$  Hz and  $f_{Aliasing}=2$  kHz, different IIR filter orders, two octaves Lagrange interpolation bandwidth.

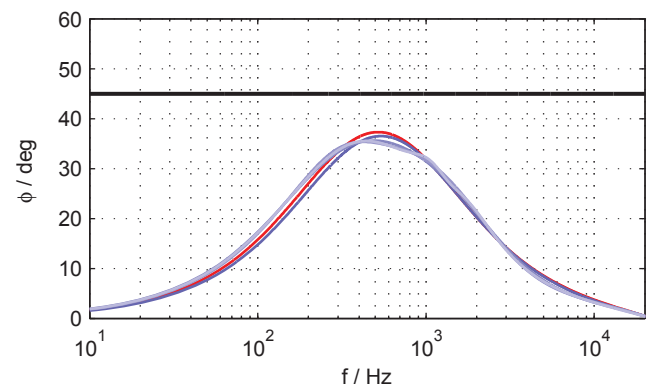


**Figure 8:** Phase frequency response for fig. 7.

A simulation of the soundfield synthesis was performed in Matlab in order to emphasize the usage of the correct phase of the prefilter from a technical point of view. A quasi-infinite and quasi-continuous SSD is considered for the numerical simulation, hence no windowing and aliasing artifacts occur in the results. The driving function [2, eq. (25)] is used to synthesize a primary spherical wavefield with the superposition of two frequencies  $f_l=343$  Hz and  $f_h=686$  Hz (i.e.  $\lambda_l=1$  m,  $\lambda_h=0.5$  m). The primary source is located 10 m behind the SSD and the listener reference line 10 m in front of

the SSD. The SSD is located on the x-axis, the target reproduction plane holds for  $y > 0$ . Three different

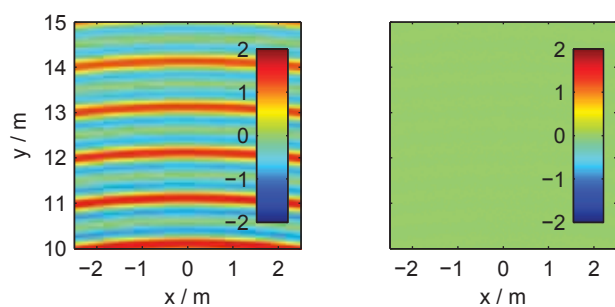


**Figure 9:** Left: soundfield synthesized with ideal prefilter phase; right: soundfield difference to ideal prefilter phase.

cases were investigated. Fig. 9 shows the usage of the ideal prefilter  $\sqrt{j\omega}$ , fig. 10 represents the soundfield employing the 4<sup>th</sup> order minimum-phase IIR filter from fig. 7 and 8. Fig. 11 results from employing a linear-phase prefilter  $|\sqrt{j\omega}|e^{-j\omega\tau}$  with chosen  $\tau = 8.3$  ms. All plots show equally normalized pressure soundfields. A delay was introduced to all prefilters. The delay was individually adapted so that exactly the same results will be obtained in all three cases when synthesizing the soundfield only for the lower frequency  $f_l$ . Thus, the

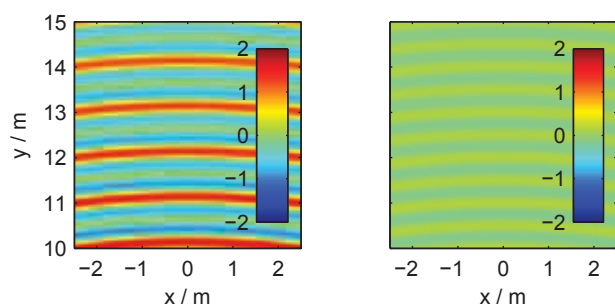


**Figure 10:** Left: soundfield synthesized with minimum-phase prefilter; right: soundfield difference to ideal prefilter phase.

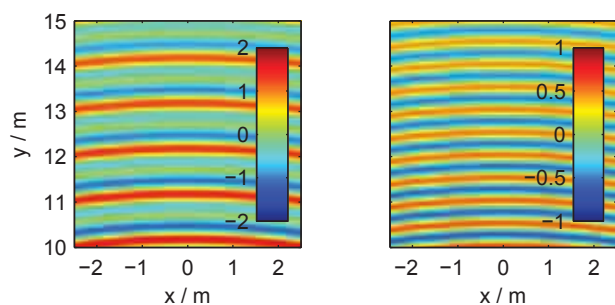


**Figure 11:** Left: soundfield synthesized with linear-phase prefilter; right: soundfield difference to ideal prefilter phase.

synthesized soundfields for the superposition of the two frequencies  $f_l$  and  $f_h$  reveal the different phase behavior of the prefilters. The ideal prefilter is used for fig. 9, and thus the two frequencies will be correctly shifted in phase by  $45^\circ$ . The minimum-phase prefilter applies a phase shift of about  $35^\circ$  to both simulated frequencies,

which results in some difference in fig. 10 compared to the ideal prefilter. For the linear-phase implementation the difference of the wavefields is large for the parameters chosen here. This is due to the fact that the linear-phase filter does not apply a constant phase-shift but rather a constant group-delay. The simulation shows that a linear-phase prefilter may not be the optimum choice.

## Conclusion

For the prefilter required in soundfield synthesis a straightforward IIR filter design method with few degrees of freedom was proposed. The filter is designed in the frequency domain, thus other driving functions known from literature could also be adapted to the occurring shelving characteristics. The filter can be customized in a simple way to different requirements and compensates for the non-ideal frequency response of a spatially sampled and finite length secondary source distribution. The resulting minimum-phase IIR filters match the amplitude response perfectly and the desired phase reasonably well in the interesting mid-frequency range. Depending on the specific application 1<sup>st</sup> to 8<sup>th</sup> order IIR filters are suitable which will reduce the computational complexity of the signal processing chain. The prefilter design method will become part of the sound field synthesis toolbox [8].

## References

- [1] Spors, S.; Rabenstein R.; Ahrens, J. (2008): "The Theory of Wave Field Synthesis Revisited". In *Proc. of the 124th AES Conv., Amsterdam*, #7358.
- [2] Spors, S.; Ahrens, J. (2010): "Analysis and Improvement of Pre-Equalization in 2.5-Dimensional Wave Field Synthesis". In *Proc. of the 128th AES Conv., London*, #8121.
- [3] Ahrens, J.; Spors, S. (2010): "Sound Field Reproduction Using Planar and Linear Arrays of Loudspeakers". In *IEEE Trans. Audio Speech Language Process.* **18**(8):2038–2050.
- [4] Barbosa, R.S.; Tenreiro Machado J.A.; Silva M.F. (2006): "Time domain design of fractional differintegrators using least-squares approximations". In *Signal Processing.* **86**(10):2567–2581.
- [5] Antoniou, A. (1993): *Digital Filters: Analysis, Design and Applications*. 2nd ed. New York: McGraw-Hill.
- [6] Salvador, C.D. (2010): "Wave Field Synthesis using Fractional Order Systems and Fractional Delays". In *Proc. of the 128th AES Conv., London*, #8122.
- [7] Olver F.W.J.; Lozier D.W.; Boisvert R.F.; et al. (2010): *NIST Handbook of Mathematical Functions*. 1st ed. Cambridge: University Press.
- [8] Wierstorf, H.; Spors, S. (2012): "Sound Field Synthesis Toolbox". In *Proc. of the 132nd AES Conv., Budapest*. Engineering Brief #50.